Supplemental material for Zhuang *et al.* report

The conformations of loops A and B of the hairpin ribozyme change along the reaction pathway.

See Fig. S1.

Docking and undocking kinetics of ribozyme-S(O'MeA-1) complexes.

From FRET time trajectories, the dwell times in the docked and undocked states were measured. The number of docking and undocking events (N) with dwell times shorter than t were determined. Two separate experiments, A with a lower time resolution (2 s) and photobleaching rate (0.001 s^{-1}) and B with a higher time resolution (0.1 s) at the expense of a higher photobleaching rate (~0.02 s^{-1}), were carried out to obtain these data. Dwell times of the undocked state from experiment A are shown in Fig. S2A. The line is a single exponential fit that gives the rate constant for docking, $k_{dock} = 0.008\ s^{-1}$. Dwell times of the docked state from experiment A are shown in Fig. 4. Dwell times of the docked state from experiment B are shown in Fig. S2B. The line is a triple exponential fit with $k_{undock,2} = 0.06\ s^{-1}$, $k_{undock,3} = 0.5\ s^{-1}$, and $k_{undock,4} = 3\ s^{-1}$.

Docking and undocking kinetics of the ribozyme-5'P and ribozyme 3'P complexes.

Using FRET, we measured the docking kinetics of the hairpin ribozyme in the presence of 5 μM 3'P and no 5'P. The ribozyme docks briefly with $k_{dock}^{3P} = 1.6\ s^{-1}$ and $k_{undock}^{3P} = 64\ s^{-1}$. In the presence of 5 μM 5'P and no 3'P, no docking event was observed.

Memory effect of the undocking kinetics.

We found that the enzyme displays a "memory" effect where the docking time of an event is highly correlated with the docking time of the previous event. A correlation analysis of the i^{th} time versus the $(i+1)^{th}$ time spent in the docked state is shown in Fig. S3. Strong correlation between adjacent docking events is unambiguously revealed in this two-dimensional histogram that shows a pronounced high occurrence frequency along the diagonal line

Dissociation equilibrium and rate constants of 3'P and 5'P in the undocked state.

Binding of 5'P alone to the ribozyme causes the FRET value to decrease from the S-free value of 0.38. At saturating concentration of 5'P (5 μM), the FRET value decreases to 0.18. At sub-saturation concentrations, the average FRET value is between 0.18 and 0.38, and the FRET time trajectories show fluctuations. The cross-correlation function of the donor and the acceptor $f(\tau) = \left\langle \left(I_{\mathrm{D}}(t) - \left\langle I_{\mathrm{D}}(t)\right\rangle_t\right)\left(I_{\mathrm{A}}(t+\tau) - \left\langle I_{\mathrm{A}}(t)\right\rangle_t\right)\right\rangle_t \Big/ \left(\left\langle I_{\mathrm{D}}(t)\right\rangle_t \left\langle I_{\mathrm{A}}(t)\right\rangle_t\right)$ was determined at a number of different concentrations of 5'P, giving the dissociation equilibrium constant $K_d^{5\mathrm{P}} = 1$ μM and rate constant $k_{\mathrm{off}}^{5\mathrm{P}} = 2\ \mathrm{s}^{-1}$.

To determine the dissociation equilibrium and rate constants of 3'P, the universal fluorescence quencher dabcyl was attached to the 3' end of 3'P (3'P-D). In the absence of 3'P-D, the FRET value between donor and acceptor on the ribozyme is ~0.38, leading to a sizable acceptor signal. The binding of 3'P-D brings dabcyl very close to the acceptor and quenches its fluorescence significantly. At a sub-saturating concentration of 3'P-D, the binding and releasing of 3'P-D causes the acceptor fluorescence to fluctuate (See Fig. S4). From the on- and off-times of the acceptor fluorescence, dissociation equilibrium and rate constants for 3'P were determined to be $K_{\mathrm{d}}^{3\mathrm{P}} = 0.2$ μM and $k_{\mathrm{off}}^{3\mathrm{P}} = 1.3\ \mathrm{s}^{-1}$, respectively.

Coupled differential equations for the enzymatic reaction of the hairpin ribozyme.

The set of coupled differential equations that describes the reactions given in Fig. 1B is as follows:

$$\frac{dN_{\mathrm{undock}}^{\mathrm{S}}}{dt} = k_{\mathrm{undock}} N_{\mathrm{dock}}^{\mathrm{S}} - k_{\mathrm{dock}} N_{\mathrm{undock}}^{\mathrm{S}} ,$$

$$\frac{dN_{\mathrm{dock}}^{\mathrm{S}}}{dt} = k_{\mathrm{dock}} N_{\mathrm{undock}}^{\mathrm{S}} + k_{\mathrm{lig}} N_{\mathrm{dock}}^{3\mathrm{P5P}} - k_{\mathrm{undock}} N_{\mathrm{dock}}^{\mathrm{S}} - k_{\mathrm{cleav}} N_{\mathrm{dock}}^{\mathrm{S}} ,$$

$$\frac{dN_{\mathrm{dock}}^{3\mathrm{P5P}}}{dt} = k_{\mathrm{cleav}} N_{\mathrm{dock}}^{\mathrm{S}} - k_{\mathrm{lig}} N_{\mathrm{dock}}^{3\mathrm{P5P}} - k_{\mathrm{undock}}^{3\mathrm{P5P}} N_{\mathrm{dock}}^{3\mathrm{P5P}} + k_{\mathrm{dock}}^{3\mathrm{P5P}} N_{\mathrm{undock}}^{3\mathrm{P5P}} ,$$

$$\frac{dN_{\mathrm{undock}}^{3\mathrm{P5P}}}{dt} = k_{\mathrm{undock}}^{3\mathrm{P5P}} N_{\mathrm{dock}}^{3\mathrm{P5P}} - k_{\mathrm{dock}}^{3\mathrm{P5P}} N_{\mathrm{undock}}^{3\mathrm{P5P}} - k_{\mathrm{off}} N_{\mathrm{undock}}^{3\mathrm{P5P}} ,$$

$$\frac{dN_{\mathrm{diss}}}{dt} = k_{\mathrm{off}} N_{\mathrm{undock}}^{3\mathrm{P5P}} .$$

Here, N^{S}_{undock} = the number of enzymes in the undocked state with S bound, N^{S}_{dock} = the number of enzymes in the docked state with S bound, N^{3P5P}_{dock} = the number of enzymes in the docked state with products bound, N^{3P5P}_{undock} = the number of enzymes in the undocked state with products bound, N_{diss} = the number of enzymes with products dissociated, k_{undock} = undocking rate constant with S bound, k_{dock} = docking rate constant with S bound, k^{3P5P}_{undock} = undocking rate constant with products bound, k^{3P5P}_{dock} = docking rate constant with products bound, k_{lig} = the chemical ligation rate constant, k_{cleav} = the chemical cleavage rate constant, k_{off} = the effective (average) dissociation rate constant of 3'P and 5'P, measured at 1.6 s^{-1} (Changing this number to 1.3 s^{-1} or 2 s^{-1} do not change the conclusion). A lower limit for the chemical ligation rate constant of $k_{lig} \geq 0.2$ s^{-1} was derived from the fact that the observed overall ligation rate is limited by docking at ~0.02 s^{-1} (Fig. 1B) (*1*), which means that the chemistry rate constant k_{lig} must be at least an order of magnitude faster than this value, or ≥ 0.2 s^{-1}.

The initial boundary conditions are that at $t = 0$, $N^{S}_{undock} = 1$, and all other states are unpopulated. The solution was obtained using Mathematica. The ratio (chemistry equilibrium constant) of $k_{cleav}/k_{lig} = 0.5$ gives a good fit. Altering this ratio by 30% produces distinctly worse fits, even if the background of not active ribozyme is allowed to vary, as shown in Fig. S5A. The fits also determine an upper limit of $k_{lig} \leq 0.8$ s^{-1}. Fig. S5B shows the results of the set of equations with $k_{lig} = 0.8$ s^{-1} while keeping $k_{cleav}/k_{lig} = 0.5$.

Fig. S1. Schematic of the reaction pathway of the hairpin ribozyme showing the induced fit between loops A and B. Substrate (S) is bound by the ribozyme (Rz) to form the undocked complex, with helices 2 and 3 co-axially stacked. This inactive intermediate needs to bend around a flexible hinge for loops A and B to interact in the docked, active conformation. FRET distances between donor and acceptor as observed in our experiments are indicated. For the loop structures of the extended and docked conformers we use a two-dimensional representation, annotated according to Leontis and Westhof (*2*), with the structures suggested by NMR (*3*, *4*) and X-ray crystallography (*5*), respectively. Substantial conformational changes in the loops accompany docking. Tertiary hydrogen bonds forming in the docked state are indicated in red, g+1-C25 Watson-Crick base pair; blue, ribose-zipper; purple, U42 binding pocket. For our studies, biotin and the fluorophores Cy3 and Cy5 were attached as indicated.

Fig. S2. Docking and undocking kinetics of ribozyme-S(O'MeA-1) complexes. (**A**) The number of undocking events (*N*) with dwell times shorter than *t* determined from experiment A. The line is a single exponential fit that gives the rate constant for docking, $k_{dock} = 0.008\ s^{-1}$. (**B**) The number of docking events (*N*) with dwell times shorter than *t* determined from experiment B. The line is a triple exponential fit with $k_{undock,2} = 0.06\ s^{-1}$, $k_{undock,3} = 0.5\ s^{-1}$, and $k_{undock,4} = 3\ s^{-1}$.

Fig. S3. Two-dimensional histogram of a pair of adjacent docked times. The color indicates the occurrence frequency. Red-orange indicates high frequency, blue indicates low frequency, and yellow and green indicate intermediate frequencies.

Fig. S4. Time trace of acceptor fluorescence of a single hairpin ribozyme in the presence of 300nM 3'P-D.

Fig. S5. Numerical solutions for the coupled differential equations for the enzymatic reaction of the hairpin ribozyme. (**A**) A comparison of various enzyme reaction curves for k_{cleav} with fixed values of k_{lig}. The background level of inactive enzymes was chosen to optimize the fit. (**B**) The reaction curves for $k_{cleav} = 0.4\ s^{-1}$ and $k_{lig} = 0.8\ s^{-1}$ compared with $k_{cleav} = 0.12\ s^{-1}$ and $k_{lig} = 0.24\ s^{-1}$.

References

1. N. G. Walter, K. J. Hampel, K. M. Brown, J. M. Burke, *EMBO J.* **17**, 2378 (1998).

2. N. B. Leontis, E. Westhof, *RNA* **7**, 499 (2001).

3. Z. Cai, I. Tinoco, *Biochemistry* **35**, 6026 (1996).

4. S. E. Butcher, F. H. Allain, J. Feigon, *Nature Struct. Biol.* **6**, 212 (1999).

5. P. B. Rupert, A. R. Ferre-D'Amare, *Nature* **410**, 780 (2001).

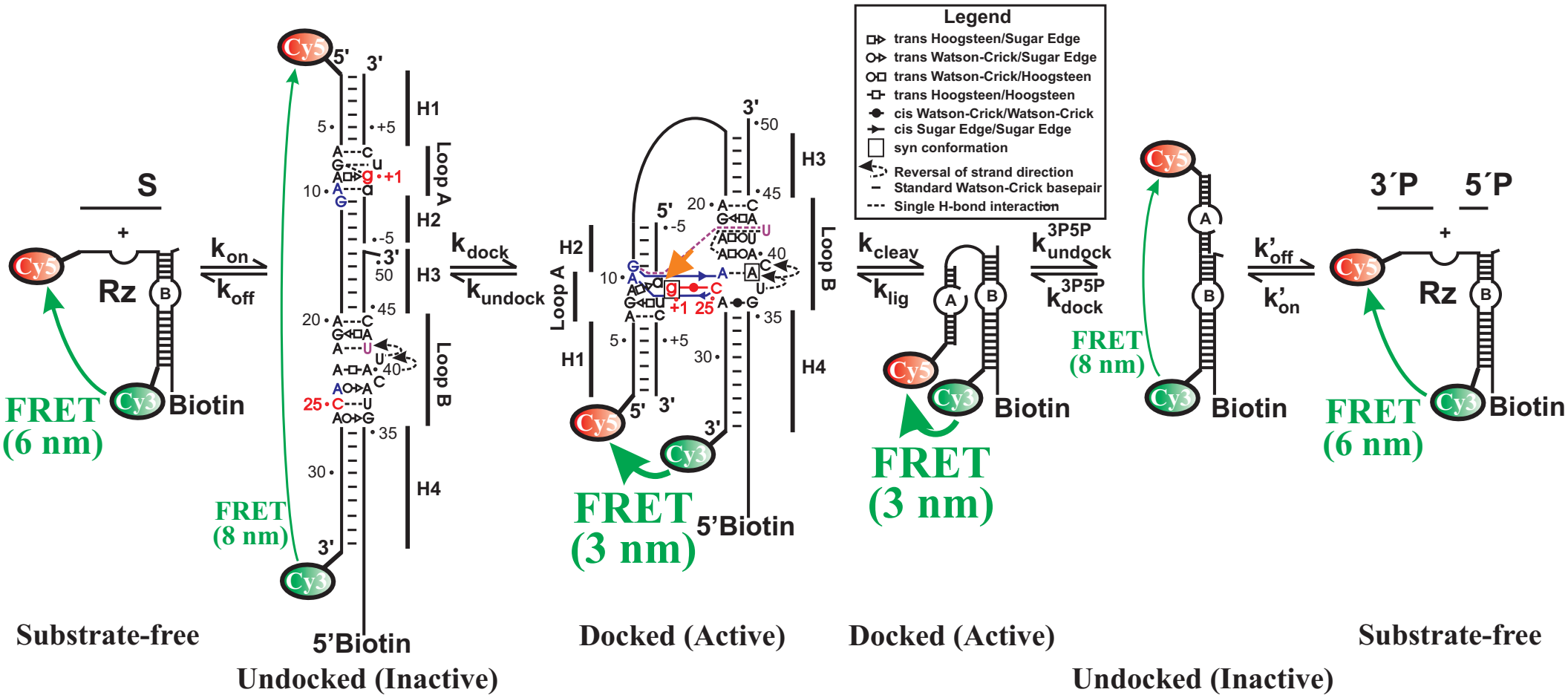

Figure S1
X. Zhuang

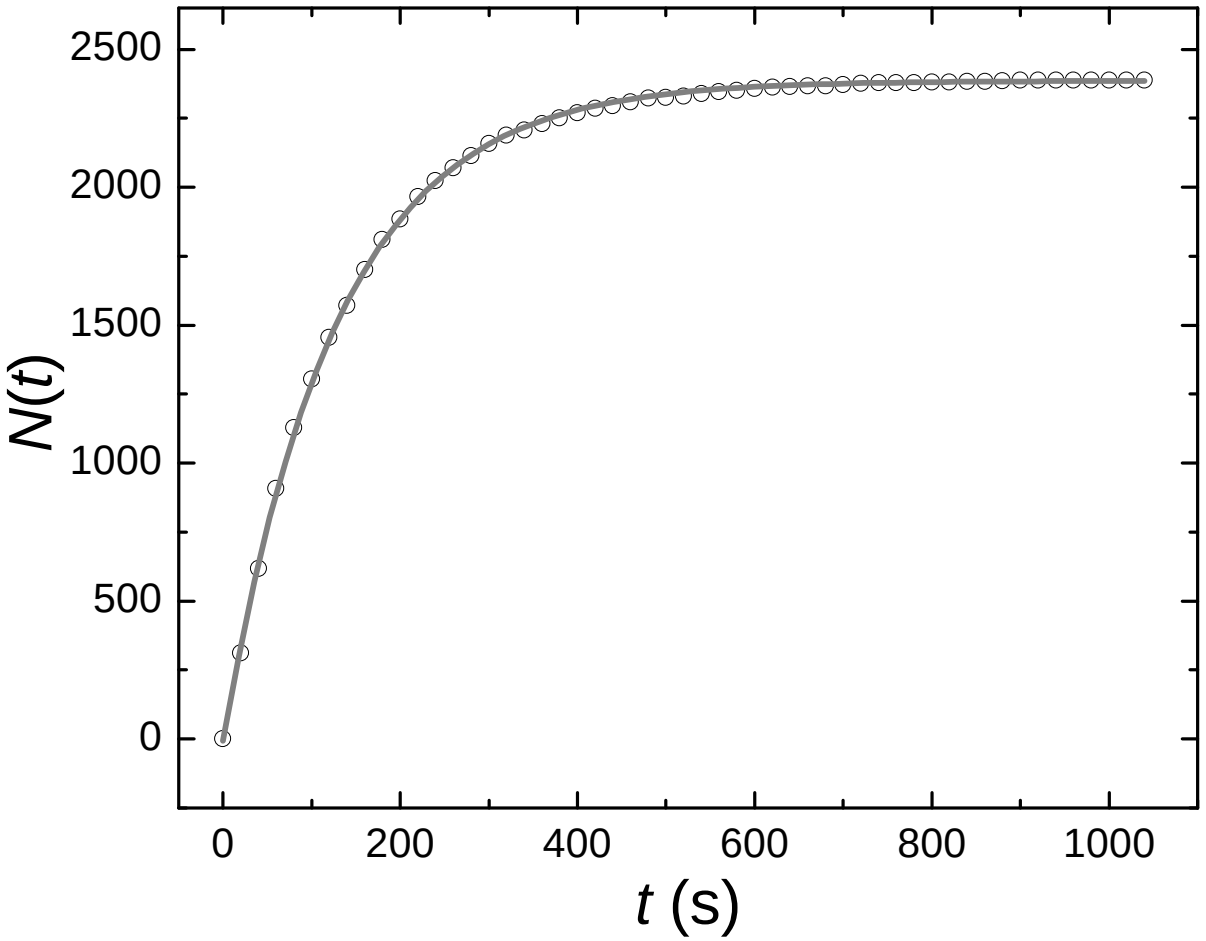

SFigure 2A
X. Zhuang

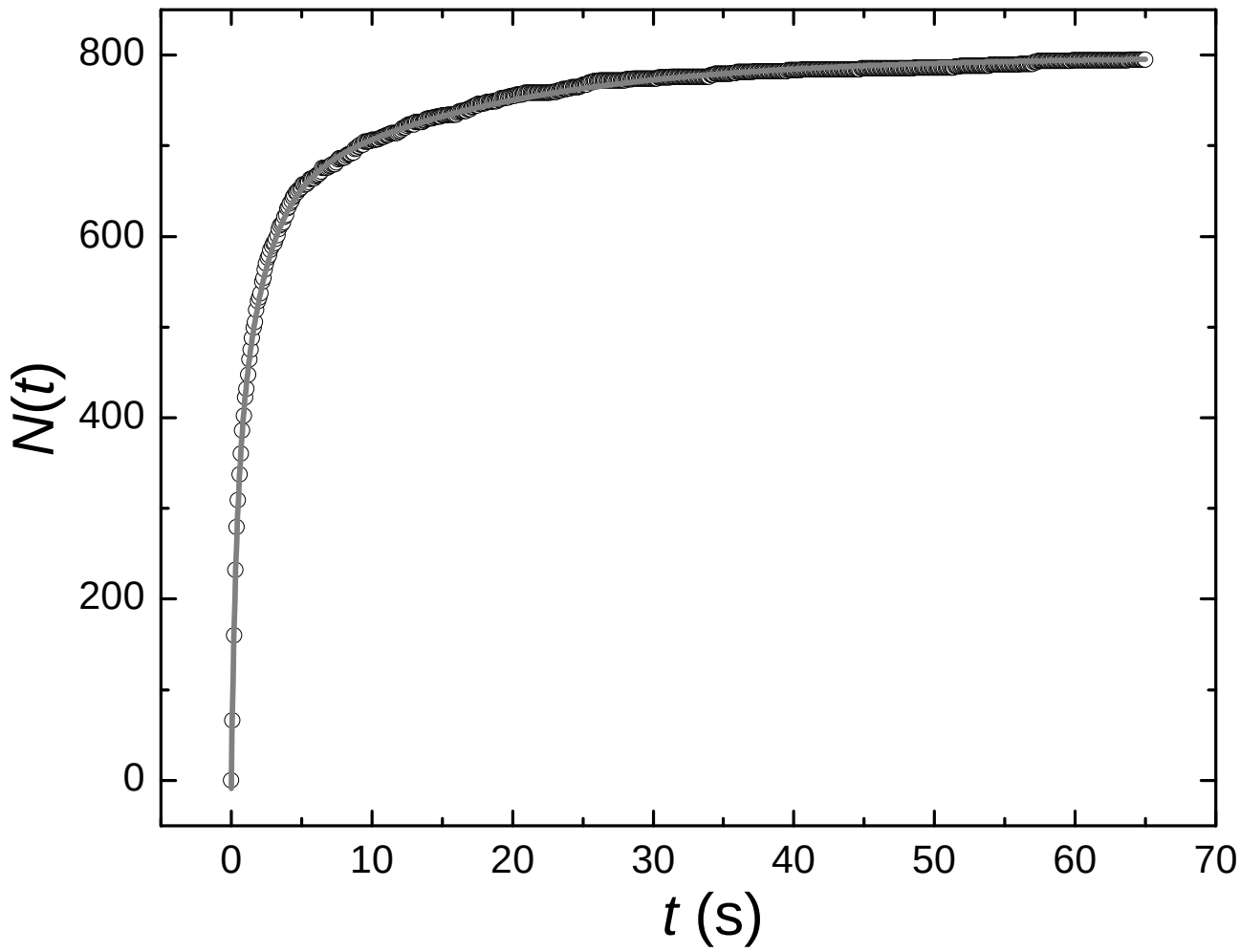

SFigure 2B
X. Zhuang

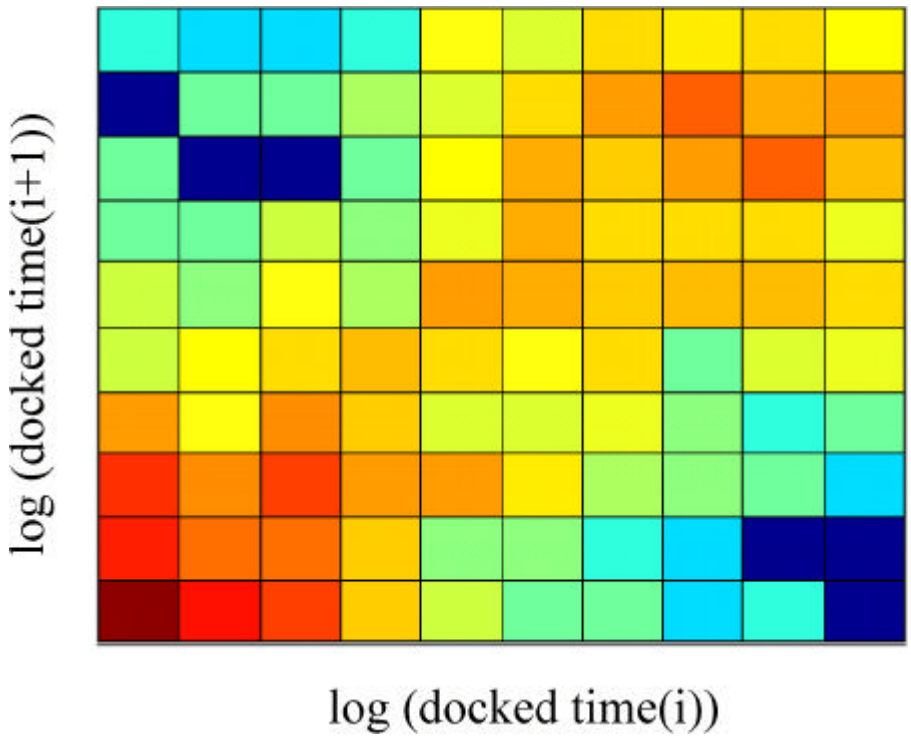

SFigure 3

X. Zhuang

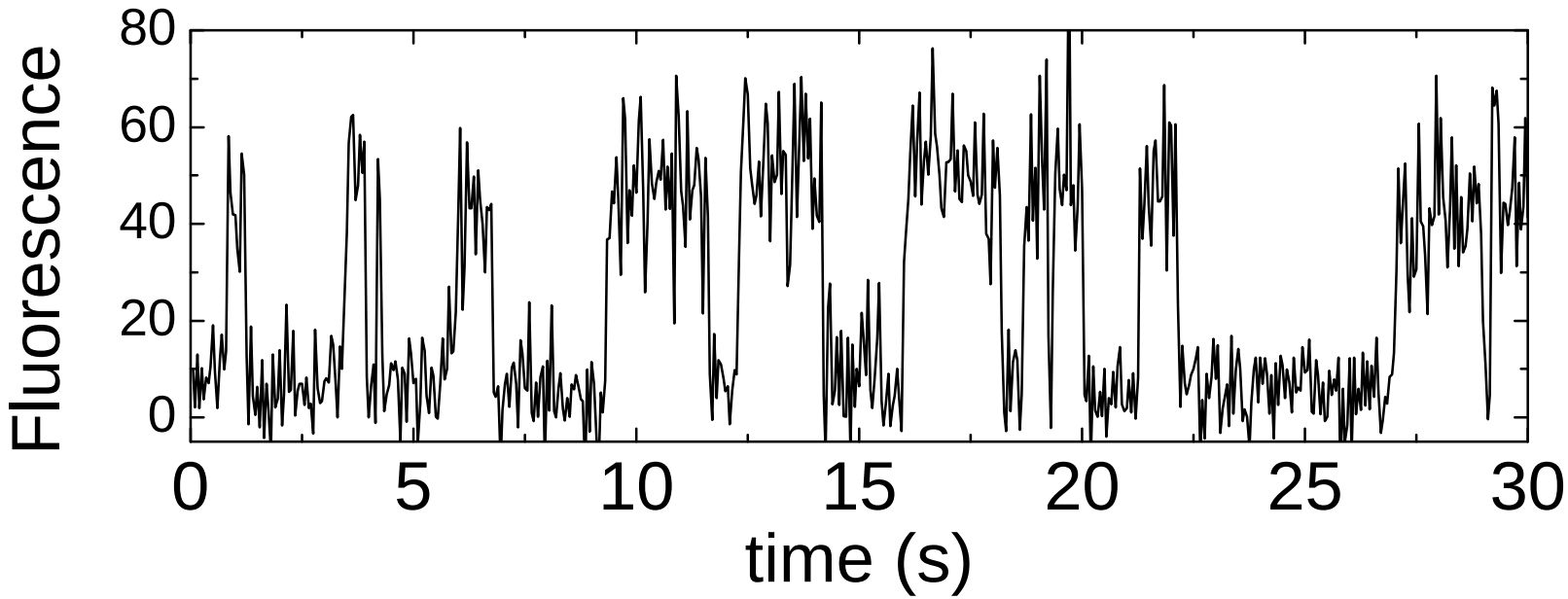

SFigure 4
X. Zhuang

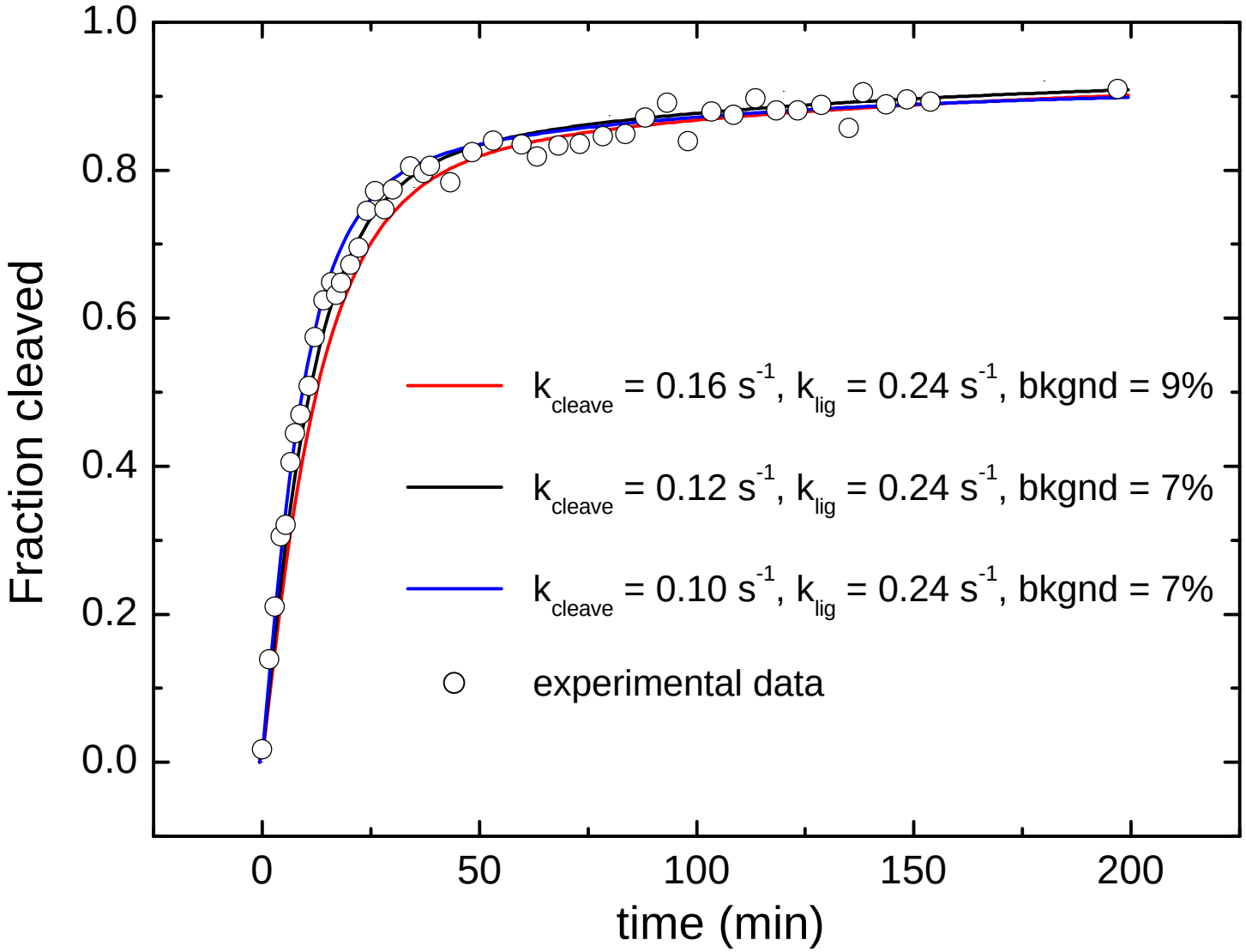

SFigure 5A
X. Zhuang

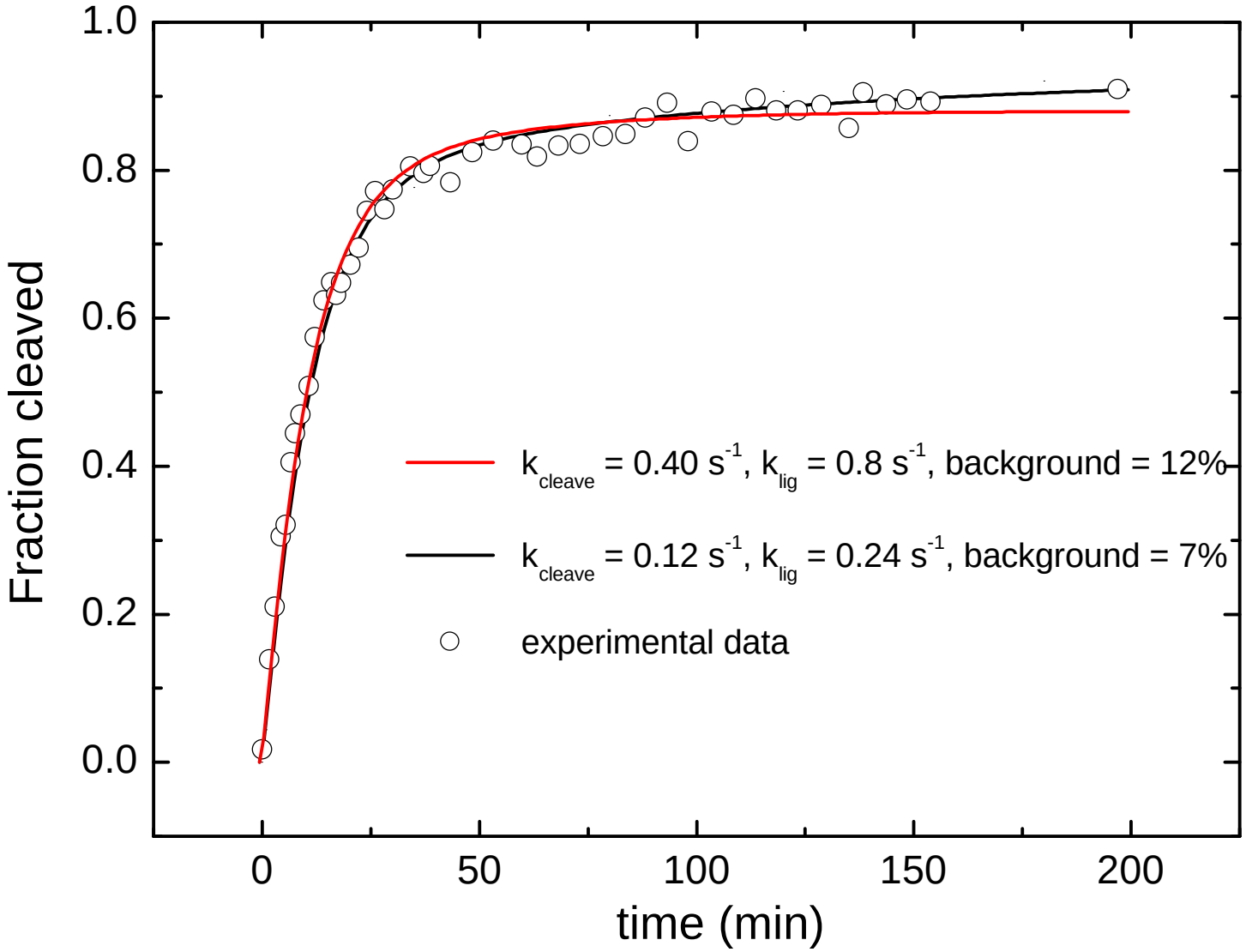

SFigure 5B
X. Zhuang